Dielectric Relaxation in Ice and Ice Clathrates and Its Connection to the Low-Temperature Phase Transition Induced by Alkali Hydroxides as Dopants

Madhusudan Tyagi and S. S. N. Murthy*

School of Physical Sciences, Jawaharlal Nehru University, New Delhi 110 067, India

Received: June 1, 2001; In Final Form: November 16, 2001

We have used dielectric spectroscopy (frequency range 10^6 to $10^{-3.0}$ Hz) and differential scanning calorimetry down to a temperature of 77 K to study the effect of alkali hydroxides as dopants on the molecular relaxation in hexagonal ice (I_h) and in clathrate hydrates (I_c) of acetone and 1,4-dioxane. A drastic fall in the relaxation times of the order of 10^7-10^{12} has been noticed in I_h and I_c doped with alkali hydroxides, namely, KOH, NaOH, LiOH, and $Ca(OH)_2$. It appears that the alkali metal- and hydroxyl-ion pairs exert a large influence on the orientational mobility of water molecules by way of polarization over a domain, and the pure phase of I_h (or I_c) is maintained outside the domains thus leading to orientational heterogeneity in the samples. The amount of phase that gets transformed to the low-temperature (low-*T*) ordered phase depends on the solid solubility of the dopant. The nature of the relaxation and variation of the static dielectric constant have been examined critically to get an insight into the actual mechanism responsible for the above events. Our studies confirm the earlier views of Tajima et al. (1984) that the low-*T* phase transition, which has so far escaped observation for kinetic reasons, has now revealed itself by the catalytic action of the dopants.

Introduction

Water exists in at least nine different crystalline forms (usually referred to as ices, that is, ice I, ice II, etc.) at different pressures and temperatures of which the first form, ice I (also referred to as hexagonal ice or I_h) is the only stable form to exist at normal pressure[1]. In addition, there are a whole range of crystalline solids called "clathrate hydrates", which are two-component systems with well-defined stoichiometry.[2−4] There is a growing interest in the study of the latter group because of their presence in interstellar molecular clouds.[5] What is much more interesting in all of these ices is the proton disorder, which leads to molecular orientation (except in ice II and ice IX)[6] and hence is categorized as one among a whole range of disordered crystals exhibiting "glasslike" phenomena.[7,8] According to the estimate by Pauling[9] on the assumption that Bernal−Fowler ice rules are strictly fulfilled, the entropy due to protons in the completely disordered configuration becomes 3.41 J/K/mol, which is in agreement with the experimental value.[10] Hence, it is expected, from the point of view of thermodynamics, that I_h will adopt a more ordered state at some temperature below 100 K. Many experiments were performed in the past on the low-temperature side below 100 K with extremely long annealing times, but what made the observance of the ordered state elusive is the kinetic factor; the relaxation of the water molecules becomes so slow even at 100 K that it requires humanly impossible time scales to observe the expected equilibrium state in pure I_h. This has led to many speculations[6,11−14] regarding the nature of the ordered state.

According to Bjerrum,[15] in pure I_h, the orientational defects generated intrinsically are responsible for the observed relaxation. He estimates the concentration of these defects at a temperature of 263 K to be of the order of $\sim 10^{-7}$ per water molecule, and this number is expected to fall drastically on lowering the temperature as their generation is an activated process. At this stage, the orientational defects generated because of the presence of unavoidable impurities are expected to dominate the relaxation process.[16,17] A considerable amount of time had been spent in the literature discussing the effects of purity and interfaces such as grain boundaries. Thus, the true nature of the relaxation in pure I_h on the lower temperature side is (always) subjective. Many attempts have been made in the past[18,19] to study the effect of dopants (intentionally added impurities) on the relaxation, in which the dopant in a quantity of the order of $10^{-7}-10^{-5}$ mole fraction is expected to form a solid solution with water molecules. Although some decrease in the relaxation time was observed, this decrease was found to be not sufficient to observe the order−disorder kind of transition expected below 100 K.

While dealing with the models of relaxation, the cubic structure of solid water is often chosen[20,21] for simplicity to represent ice I_h because of many structural similarities between the two.[22,23] The cubic form of ice is metastable with respect to ice I_h and gets irreversibly transformed during heating to ice I_h, above a temperature of 163 K. The dielectric[23] and enthalpy[24] relaxation measurements made below 163 K on cubic ice indicated no differences in cubic ice and ice I_h. The greater stability of the cubic structure due to the enclathrated molecules as in clathrate hydrates gives us a good opportunity to study these systems in greater detail up to 273 K. The enclathrated molecule in these hydrates introduces additional Bjerrum defects in the surrounding water lattice, and hence, the relaxation is accelerated.[2,4] Of all of the disordered ices and clathrate hydrates, I_h (or cubic ice) is the slowest to relax, and hence, the relaxation rates of the water lattice in clathrate hydrates are often compared with that of I_h. Interesting correlations have been reported[2,25] between the increase in the relaxation rate and the dipole moment of the enclathrated molecule. Despite the large increase in the acceleration of the relaxation, the expected low-

* To whom correspondence should be addressed. E-mail: ssnm0700@mail.jnu.ac.in.

10.1021/jp012097x CCC: $22.00
Published on Web 05/01/2002

TABLE 1: Details of Low-Temperature Transition

	dopant	dopant conc	transition temp (K)	ΔS^a	(ΔS/3.41) × %	ref
I_h	KOH	1.8×10^{-5}	71.6	−0.64	18.8	28
		1.8×10^{-4}	71.6	−1.85	54.3	28
		1.8×10^{-3}	71.6	−2.33	68.3	28
	RbOH	1.8×10^{-3}	71.6	−0.82	24	28
I_c(ACN)	KOH	1.8×10^{-4}	46.6	−2.48	72.7	30

[a] In J K^{-1} $(H_2O\text{-mol})^{-1}$.

temperature ordered state was not observed even in these systems.[2,26,27]

However, a different result was observed by Tajima et al.[28] when I_h is doped with alkali hydroxides in a mole fraction of the order of $\sim 10^{-3}$. For the sake of convenience of discussion, we have tabulated results of their specific heat (C_p) data[28−30] measurements and the corresponding thermodynamic parameters of interest in Table 1. There is a proton-ordering transition of first order at 71.6 K in I_h that is independent of the nature of dopant. The fraction transformed to the low-temperature (low-*T*) phase depended on the concentration of the dopant, and up to (only) a maximum of ∼75% of the entropy is lost after the transition to the low-*T* phase (Table 1). Similar observations have been made in acetone, tetrahydrofuran, and trimethylene oxide clathrate hydrates.[29−31] The dielectric study[27,32−36] on some of these systems, though not complete, indicates that the relaxation time of water molecules decreases by a very large factor leading to the observation of the low-*T* transition. Though this has been attributed to the catalytic action of the dopant, what is not clear is the reason for not observing a 100% loss of entropy during the transition to the low-*T* phase and the exact nature of the mechanism. In this study, we have tried to get these points clarified by critically examining these systems using dielectric spectroscopy.

Experimental Section

The water used in the study is obtained from M/s. E. Merck India, Pvt. Ltd. and is of HPLC quality with resistivity >15 MΩ. The hydroxides used in the study, potassium hydroxide (KOH), sodium hydroxide (NaOH), lithium hydroxide (LiOH), and calcium hydroxide ($Ca(OH)_2$), are obtained from M/s. s.d. fine chemicals, India, and are of analar grade.

The main technique used is that of dielectric spectroscopy, in which a HP4284A precision LCR meter (frequency range 20 Hz to 1 MHz) and a dc step response technique (frequency range $10^{-0.5}$−$10^{-3.0}$ Hz) have been used. A three-terminal liquid dielectric cell similar to the earlier one has been used. The differential scanning calorimetry (DSC) measurements are made using a DuPont TA2000 thermal analyzer using the quench cooling accessory. For the other experimental details, the reader may consult our earlier publication.[4]

Results

The dielectric studies on pure I_h have shown that the peak-loss frequency, f_m, varies[34,37] as

$$f_m = f_0 \, e^{-E/(RT)} \tag{1}$$

where f_0 is the preexponential factor and the corresponding activation energy is about ∼53 kJ/mol. However, deviations from eq 1 are noticed below $T < 220$ K, and the dielectric spectrum no longer follows the Debye behavior. Instead, the dielectric relaxation is found to follow the Cole−Cole type of behavior[37] given by

$$\epsilon^*(f) - \epsilon_\infty = \frac{(\epsilon_0 - \epsilon_\infty)}{\left[1 + i\left(\frac{f}{f_m}\right)^{1-\alpha_{cc}}\right]} \tag{2}$$

where f_m is the peak-loss frequency and ϵ_0 and ϵ_∞ are the limiting dielectric constants. The parameter α_{cc} signifies the symmetric distribution around f_m (and the Debye behavior corresponds to $\alpha_{cc} = 0$ in eq 2). The above deviations for $T < 220$ K are attributed to a switch over from an intrinsic- to an extrinsic-defect mechanism. Our data[34] on pure I_h exactly tallied with others' data[17,32] and are in agreement with the single-crystal data of Kawada.[12] Further deviations, if any, on the low-*T* side from the above single-crystal data can be attributed to the polycrystalline nature of the sample.[34] With this a priori information on pure I_h, we have started the measurements on I_h doped with alkali hydroxides.

(a) Measurements on I_h Doped with Alkali Hydroxides. All of the alkali hdyroxides studied here are found to mix well with water at the desired concentrations at room temperature. The samples are prepared gravimetrically (in the discussion below, x_m refers to the mole fractions of the alkali hydroxide in the solution prior to freezing). The dielectric cell filled with this solution is cooled slowly to form doped I_h in situ. Care has been taken to minimize the contraction of the sample between the electrodes by cooling it very slowly at a rate of about 0.5 K/min. The sample initially was held at a temperature of about 240 K for 2−3 h after which it was recycled twice between 240 and 100 K to allow the unfrozen liquid (if any) to crystallize. Then, the sample is annealed at about 240 K for 4−5 h before starting the dielectric measurements. Of all of the alkali hydroxides, KOH was specially chosen for study at various x_m values because of the a priori information about the specific heat data (Table 1) and the liquid−solid phase diagram[28] on the aqueous mixtures of KOH. The x_m values for aqueous solution of $Ca(OH)_2$ used in the study could not be determined because some amount of $Ca(OH)_2$ always precipitated and are approximated to be between 10^{-4} and 10^{-5}.

We have studied the relaxation of I_h doped with KOH ($x_m = 3.4 \times 10^{-5}$, 3.9×10^{-4}, 2.1×10^{-3}), NaOH ($x_m = 1.37 \times 10^{-3}$), LiOH ($x_m = 1.93 \times 10^{-3}$), and $Ca(OH)_2$ ($10^{-5} \le x_m < 10^{-4}$). The general relaxation behavior is shown in Figures 1 and 2. At a low concentration of $x_m = 3.4 \times 10^{-5}$, the dielectric loss at 1 kHz test frequency shows two clearly resolved processes; the magnitude of the low-*T* process increases with x_m (Figure 1). (However, at this point, we must admit that we were not able to resolve the high-*T* process except for the case where $x_m = 3.4 \times 10^{-5}$ (Figure 3) because it is buried under large ionic polarization). The corresponding C−C diagrams in Figure 2 show an unusual skewing on the lower frequency side and hence cannot be fitted to eq 2. Shown in Figure 3 is the corresponding Arrhenius diagram, in which the peak-loss frequency, f_m, values obtained with different dopants are represented in the same plot along with the data[34] obtained for pure I_h. In Figure 4, the variation of the static dielectric constant ϵ_0 with $1/T$ is depicted for the cases for which we were able to determine its value from the C−C diagrams. However, in the rest of the cases not presented in Figure 4, we found it difficult to determine ϵ_0 because of the skewing of C−C diagrams on the lower-*F* side and also because of the presence of large ionic polarization. The large error bars in the data shown in Figure 4 are primarily due to these reasons. Some time-dependence was observed initially on the lower-*T* side probably because of premonitory effects.[28−30]

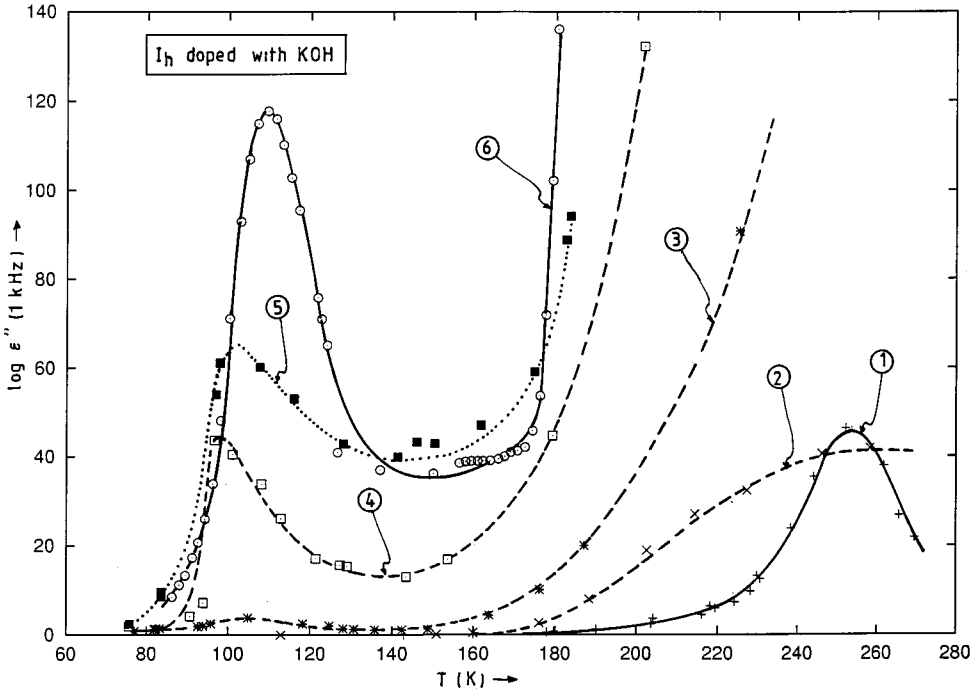

Figure 1. Temperature variation of ϵ'' at 1 kHz test frequency in I_h doped with KOH for various x_m values. The curves refer to samples with x_m = (1) 0.00 (pure I_h), (2) 5.00×10^{-6}, (3) 3.40×10^{-5}, (4) 3.95×10^{-4}, (5) 2.10×10^{-3}, and (6) 8.15×10^{-3}.

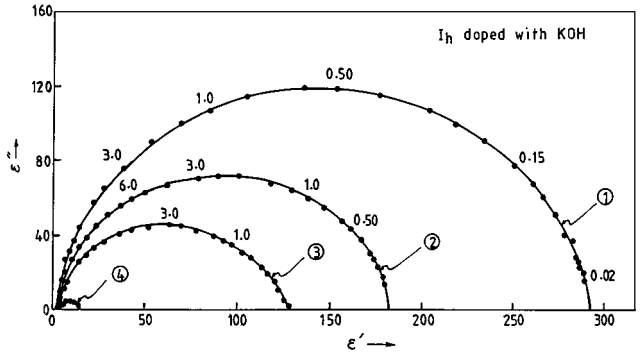

Figure 2. C-C diagrams corresponding to the relaxation of I_h doped with KOH for various x_m values. (The frequency range corresponds to 20 Hz to 1 MHz). The curves refer to samples with x_m and T values of (1) 8.15×10^{-3}, 107.1 K; (2) 2.1×10^{-3}, 107.6 K; (3) 3.95×10^{-4}, 108.0 K; (4) 3.4×10^{-5}, 94.0 K. The numbers beside the experimental points correspond to the frequency in kHz.

(b) Measurements on Clathrate Hydrates Doped with Alkali Hydroxides. Clathrate hydrate (I_c) possesses an additional disorder over I_h associated with the enclathrated molecules.[2,14] It is with this interest in mind that we have studied the acetone (ACN) clathrate hydrate [I_c(ACN)] doped with alkali hydroxides. The undoped I_c(ACN) was very well-studied by us recently.[4] For the sake of convenience of discussion, we refer the reader to the liquid−solid phase diagram (PD) shown in ref 4. The composition of this clathrate hydrate is A·17H_2O. The PD is eutectic at 177.5 K with incongruent melting at 253.2 K and a peritectic transition at 258.2 K. The solutions are prepared gravimetrically by dissolving the alkali hydroxide in an aqueous solution of above composition (A·17H_2O), and the samples are then prepared in situ as specified in the case of I_h described in the preceding section.

Dielectric relaxation measurements were previously reported for this system doped with KOH over a wide temperature range of 20−250 K by Yamamuro et al.[36] These authors observed that the dielectric dispersion associated with water reorientation disappears suddenly at the transition temperature, 46.6 K (Table 1), and no more dielectric dispersion was observed below that temperature. The above measurements were made at only one doping level of KOH with $x_m = 1.8 \times 10^{-4}$ because the focus was on the ordering transition. Here, we have taken measurements on the samples over a wider range of doping levels of KOH and also with different dopants. Shown in Figure 5 are the DSC curves in the region of the clathrate decomposition temperature for both the pure and doped hydrate, which clearly revealed the existence of clathrate hydrate up to at least a value of $x_m = 1.1 \times 10^{-3}$. The corresponding C−C diagrams are shown in Figures 6 and 7. As in the case of I_h doped with small amounts of KOH (Figure 1), there are two processes even in the case of clathrates (for the sake of convenience hereafter, we wish to refer to the high-T (low-F) and low-T (high-F) processes as process I and II, respectively). This situation in shown in Figure 7 in the form of C−C diagrams. The f_m values determined for the doped samples are given in Figure 8 along with that of the undoped sample. The corresponding T variation of the static dielectric constant is shown in Figure 9.

We have also studied the clathrate hydrate of dioxane [I_c-(DXN)] using various dopants. The liquid−solid phase diagram of the water−DXN system (without dopants) is eutectic with an incongruent melting transition at 259.7 K and with a solid−solid transition in dioxane at 272 K (refer to Table 1 of our earlier publication[4]). The above specified incongruent melting transition temperature refers to the decomposition temperature of DXN hydrate. This clathrate hydrate has an approximate composition of A·17H_2O and is a type II hydrate.[4] Our DSC studies confirmed the existence of the clathrate hydrate in samples doped with the alkali hydroxides the decomposition temperature of which was found to be the same as that of the undoped samples. The formation of doped hydrate in this case required prolonged annealing probably because the dioxane molecule is too big for the cavities of the ice clathrate.[2,38] The amount of doped hydrate, hence, was found to depend on annealing time, and even after a day of annealing, the transformation was found to be incomplete. The C−C diagram

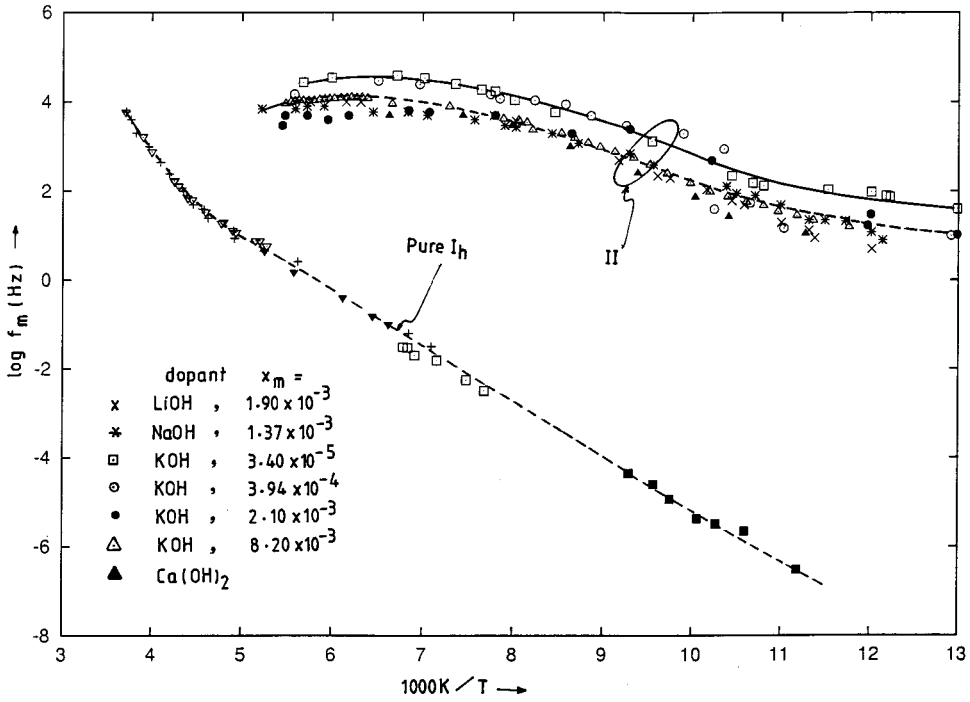

Figure 3. Variation of f_m of doped I_h with temperature. Also shown in the figure are the pure I_h values for comparison. The data corresponding to pure I_h are taken from Murthy[34] (+), Worz and Cole[17] (▽), single-crystal data of Kawada[12] (▽), and enthalpy relaxation data of Haida et al.[10] (■). Note that process I corresponding to the KOH concentration of 3.40×10^{-5} falls along that of pure I_h (shown by ⊡ along the data of pure I_h). The lines through the experimental points are a guide to the eye.

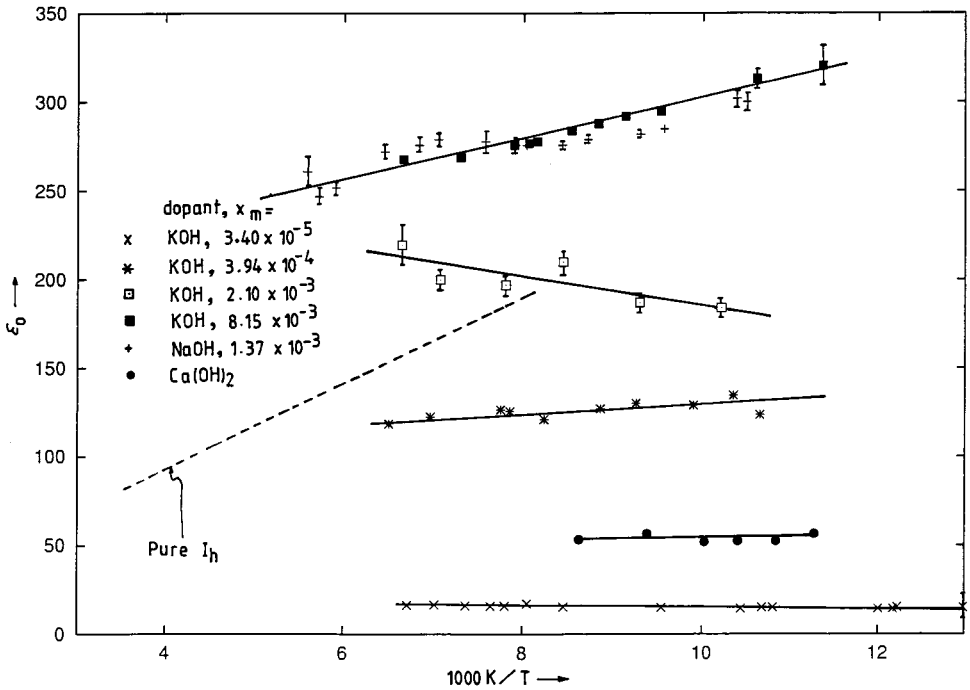

Figure 4. Temperature variation of the static dielectric constant ϵ_0 of doped I_h. The dashed line corresponds to single-crystal data of Kawada[12] and our polycrystalline data on pure I_h and I_h doped with nonelectrolytes, all of which are approximately located around the dashed line (see ref 34 for further details on pure I_h).

for the DXN hydrates doped with alkali hydroxides is similar to that shown in Figure 2. The corresponding relaxation rates are shown in Figure 10 along with those of the pure hydrate. The values of ϵ_0 are always found to vary with annealing (with more or less no change in f_m), especially with KOH as dopant (not shown in any diagram). The ϵ_0 values are found to be of the magnitude of 154 for NaOH-doped samples, but in cases of KOH and LiOH, they dropped to 55 and 20, respectively, for the same amount of annealing indicating that the doping/clathrate formation is not complete. This aspect requires further investigation.

We have critically examined the high-frequency side of the relaxation process for which we preferred to plot the loss data against the frequency as shown in Figure 11.

Discussion

For the sake of convenience, we have split the discussion into a number of points as given below.

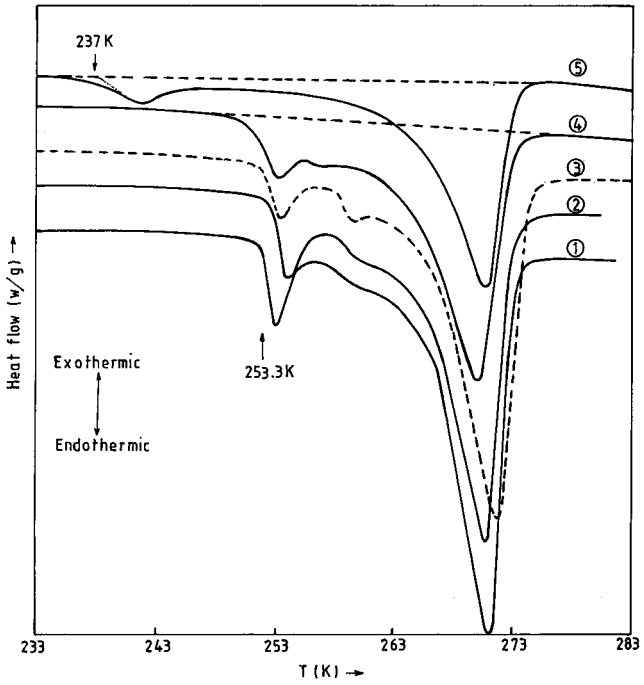

Figure 5. DSC curves for water−ACN binary system corresponding to the clathrate composition $x_m = 0.055$ for a heating rate of 2°/min: (1) pure water−ACN system (sample weight = 8.0 mg); (2−5) water−ACN system doped with KOH with x_m and sample weights of (2) 3.9×10^{-5}, 9.2 mg; (3) 1.36×10^{-4}, 8.5 mg; (4) 9.0×10^{-4}, 10.1 mg; (5) 9.6×10^{-3}, 9.9 mg. The curves are shifted downward with reference to curve 5 for the sake of clarity.

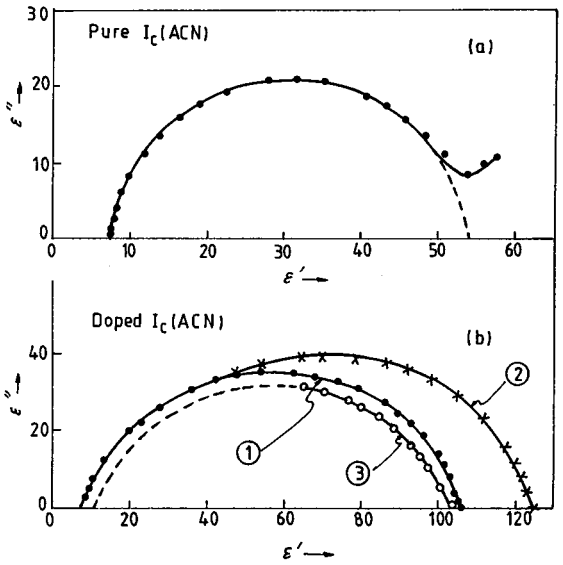

Figure 6. C−C diagram corresponding to the relaxation in I_c(ACN): (a) pure (T = 163.9 K); (b) doped with (1) LiOH ($x_m = 1.1 \times 10^{-3}$), $T = 80.6$ K; (2) NaOH (1.37×10^{-3}), $T = 77.4$ K; (3) KOH (2.2×10^{-3}), $T = 77$ K. The frequency range is 20 Hz to 1 MHz.

(a) The Peak-Loss Frequency, f_m. A quick look at the compiled data of relaxation times of pure clathrate hydrates (as given in Table 4 of ref 25) reveals that the relaxation of water molecules is accelerated by many-fold. This is also clear by comparing the data of Figure 8 with that of Figure 3 for the pure phases in which one can see that the acceleration increases more on the low-T side. In this connection, one is tempted to ask why the low-T ordered phase is not observed in clathrate hydrates despite the above-mentioned acceleration. The answer mainly lies in the lowering of the transition temperature

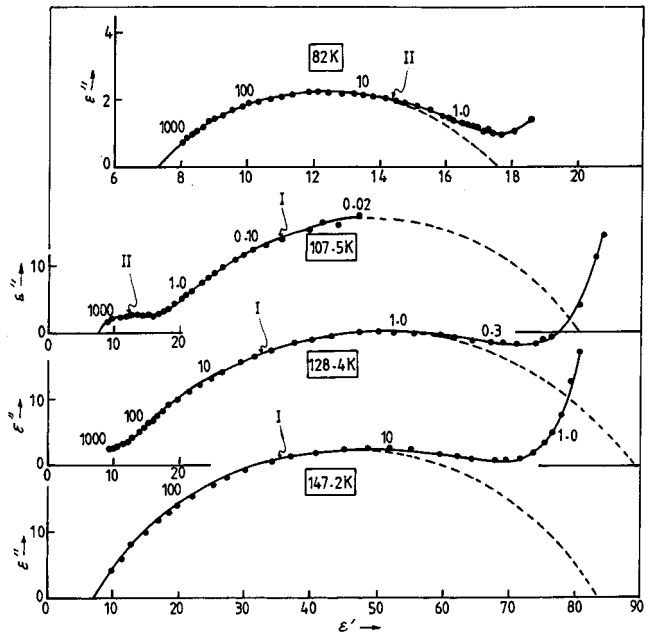

Figure 7. C−C diagrams for I_c(ACN) doped with KOH ($x_m = 7.48 \times 10^{-5}$) at various temperatures. The numbers beside the experimental points correspond to frequency in kHz. Note that with increase in temperature in addition to the low-T process (referred to as process II) another process (designated as process I) of much larger intensity dominates the relaxation.

corresponding to the low-T ordered phase. If we take, for example, the case of I_c(ACN), the transition temperature (Table 1) is lowered to 46.6 K from 71.6 K in I_h (both of which are independent of the dopants and hence are to be treated as the equilibrium properties of the material in question[28−30]). This lowering of transition temperature is expected because of the weakened intermolecular forces in the water lattice due to the presence of the enclathrated molecule, which is generally not bonded to the water molecules.[2−4] Extrapolation of the Arrhenius curve of pure I_c(ACN) shown in Figure 8 down to 46.6 K reveals that the f_m value at 46.6 K is of the order of 10^{-10} or equivalently about 50 years in time. This time scale may increase further if the Arrhenius curve starts changing rapidly on the lower temperature side, which is not uncommon in ices.[13,14,34] Thus, we see that the observation of the low-T ordered phase even in pure ice clathrates is highly unlikely because of kinetic reasons as in the case of pure I_h discussed in the Introduction.

The situation changes quite drastically when the ice I_h and ice clathrates are doped with alkali hydroxides. The peak-loss frequency f_m at 77 K increases by $10^7-10^{9.5}$ times in I_h doped with alkali hydroxides in comparison to that of the pure I_h (Figure 3). The increase in f_m is $10^{10}-10^{12}$ times in the case of I_c(ACN) (Figure 8) and is about $10^{7.5}$ times in the case of I_c-(DXN) (Figure 10) against their respective pure phase f_m values at 77 K. These observations are very much similar to the ones made by Yamamuro et al.[35,36] in the case of tetrahydrofuran, trimethylene oxide, and acetone clathrate hydrates doped with KOH of $x_m = 1.8 \times 10^{-4}$. Such a large increase in f_m values was not observed[34] in I_h doped with nonelectrolytes. It is very clear that the increase in the f_m values (or reduction in the relaxation times) by doping with alkali hydroxides is responsible for the observation of first-order events at 71.6 K in I_h and 46.6 K in I_c(ACN) (Table 1).

There is a tendency for an increase in the f_m values for a given concentration of the dopants and with the size of the alkali ion, which can clearly be seen in the case of I_c(ACN) (Figure 8). Because it is expected that OH^- ion would take a regular

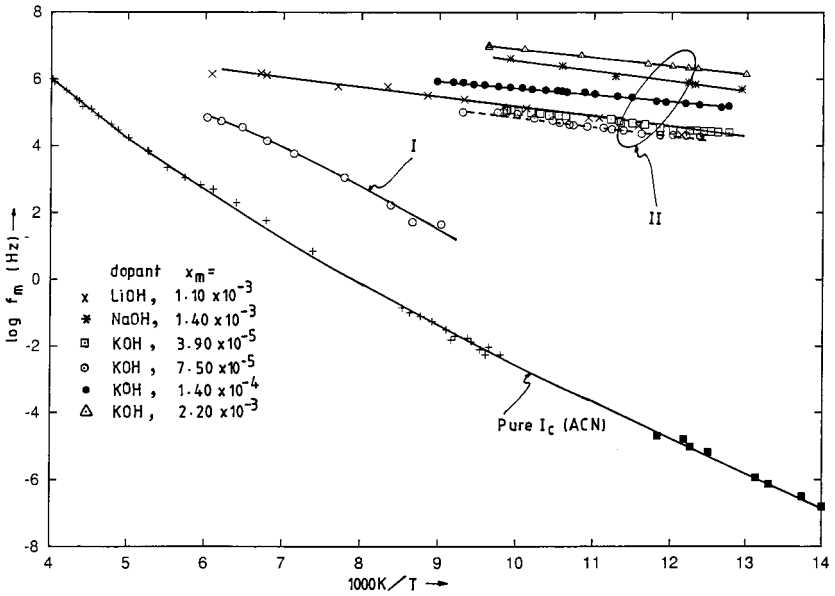

Figure 8. Temperature variation of f_m for doped I_c(ACN). The symbols (■) on pure I_c(ACN) are the enthalpy relaxation data of Kuratomi et al.[26] and the data shown by (+) are from Murthy.[4]

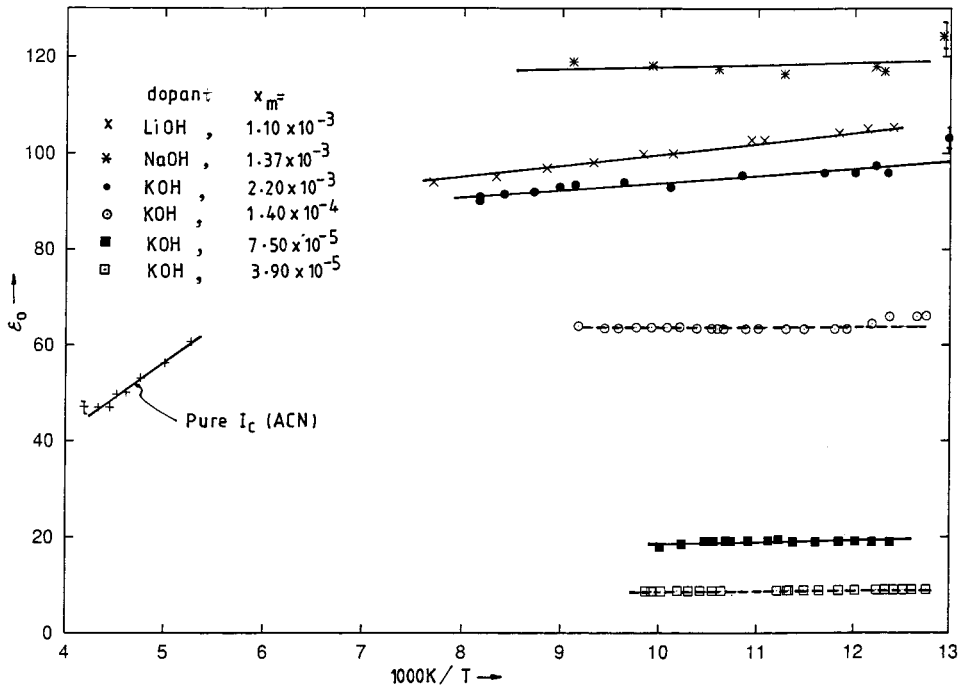

Figure 9. Temperature variation of ϵ_0 of process II in I_c(ACN) doped with various alkali hydroxide. Also shown in the figure are the data[4] corresponding to that of pure I_c(ACN) for comparison.

site on the ice lattice with the alkali (+) ion taking up some interstitial position, what is probably causing this increase in f_m value is the lattice distortion associated with this alkali ion at the interstitial site. It is also interesting to note that even though the miscibility of the second group (alkaline earth metal) hydroxides with water, both in the liquid and solid phases, is expected to be very small, still one of the hydroxides, $Ca(OH)_2$, is found to be as effective as LiOH (Figure 3). We have also tried to see the effective roles of OH^- ion and alkali (+) ions, by doping I_h with KCl and NH_4OH, but we did not find such large changes in the f_m values from that of pure I_h (see ref 34 for further details).

(b) Evidence for Orientational Heterogeneity in the Doped Sample. From Figures 1, 3, 7, and 8, it is very clear that the total polarization is split between the processes I and II, the latter of which is obviously due to the presence of alkali hydroxide in the lattice. Though one can see a clear process I in Figures 1 and 3 corresponding to a concentration of $x_m = 3.4 \times 10^{-5}$, its resolution at higher concentrations is masked for two reasons: (i) large ionic polarization and (ii) its tendency to decrease in magnitude with increasing x_m (the reader may consult ref 34 for more details on this aspect). It may also be noted that the f_m values corresponding to the process I are located along the log f_m vs $1/T$ curve corresponding to those of pure I_h (Figure 3) (or closer to those of the corresponding pure hydrate (Figure 8)). Thus, it is tempting to visualize the doped sample as the one having two regions of different orientational mobilities: one in which the water molecules are polarized because of the presence of ionic impurities and hence tend to generate orientational defects that are spatially distributed in a

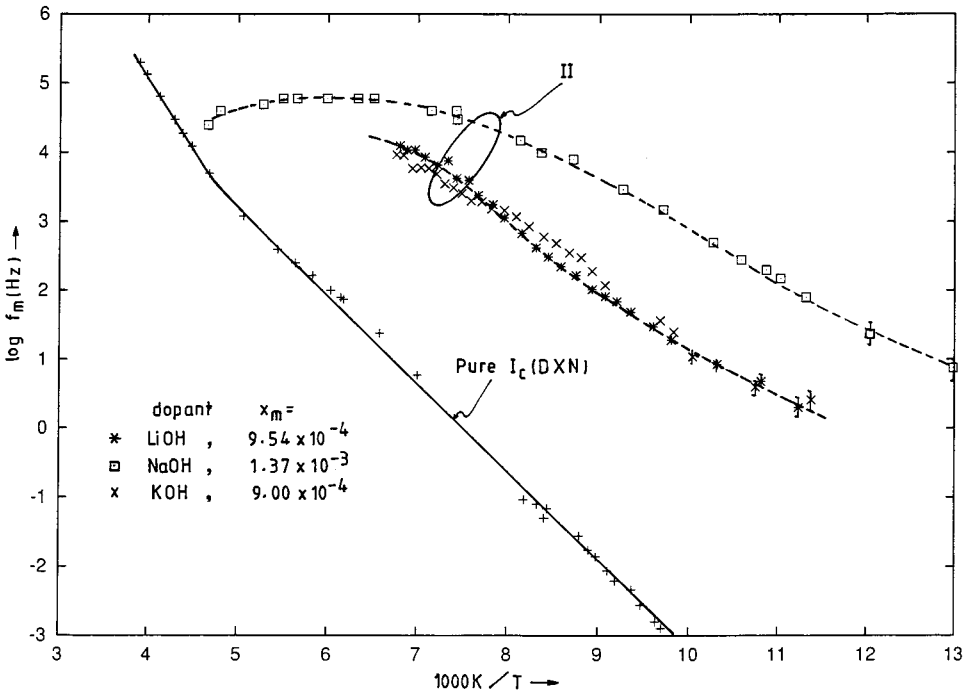

Figure 10. Temperature variation of f_m for DXN clathrate hydrate, I_c(DXN), for pure[4] sample and for the sample doped with alkali hydroxides.

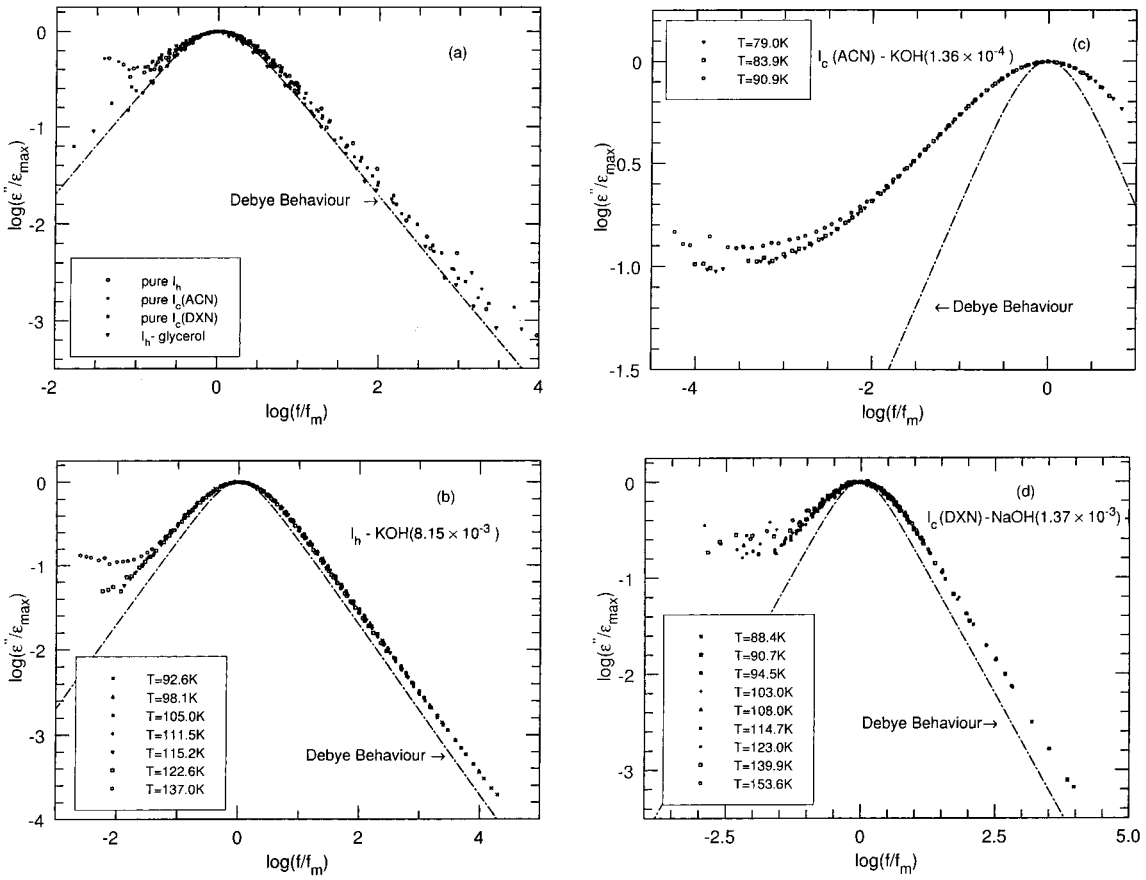

Figure 11. Variation of $\log(\epsilon''/\epsilon''_{max})$ vs $\log(f/f_m)$ at various temperatures in (a) pure samples of I_h (for $T = 229.8$, 238.4, and 244.2 K), I_c(ACN) (for $T = 147.4$, 156.2, and 163.9 K) and I_c(DXN) (for $T = 165.7$, 171.5, 197.5, and 183.7 K)). Also included is the data[34] of I_h doped with glycerol ($x_m = 6.80 \times 10^{-3}$) (for $T = 153.4$, 172.5, 182.7, 190.2, 199.5, and 209.9 K): (b) doped I_h; (c) doped I_c(ACN); (d) doped I_c(DXN). Also shown is the Debye behavior for comparison.

nonuniform fashion leading to a distribution of relaxation times and the other in which the original pure I_h (or I_c) phase is maintained (interestingly, both of the phases melt or decompose at the same temperature corresponding to that of the pure phase[28,29] as shown in Figure 5). With increase in the concentration level of dopants on the I_h (or I_c) lattice, more and more water molecules are expected to relax by process II, and process I is expected to diminish in size. This explains the increase of the static dielectric constant ϵ_0 with x_m shown in Figures 4 and 9. From Table 1 and Figure 4, one can see a qualitative

agreement in the $\Delta\epsilon$ ($\epsilon_0 - \epsilon_\infty$) values corresponding to process II and the amount of material that had transformed to the lower-*T* phase at 71.6 K. Thus, in principle, one can expect that with a further rise in x_m values the entire material would collapse to the low-*T* phase. However, because of the incompatibility between the sizes of water and KOH molecules, the solid solubility of KOH in I_h (or I_c) is limited to somewhere between $x_m = 10^{-4}$ and 10^{-3}. Therefore, the ultimate solid solubility of alkali hydroxide is important because it would decide the amount of entropy that would be removed by the low-*T* transition. Any excess of KOH above this limit, would precipitate as pure KOH at the eutectic temperature of 210.8 K.[28]

In the case of aqueous mixtures of ACN, any excess of KOH above the solubility limit is expected to be in equilibrium with the doped I_c(ACN) below 253.2 K and the corresponding liquid−solid equilibrium is expected to be very complex because it involves a three-component system. This may get much more complicated if the hydrate is unstable in the presence of large amounts of alkali hydroxide. It is with this in mind that the DSC scans in Figure 5 should be looked at. Our preliminary dielectric investigation of I_c(ACN) doped with KOH of 9.6×10^{-3} indicated a collapse of process II. It requires further investigation to ascertain the stability of clathrate hydrate at large doping concentrations. Interestingly, the corresponding DSC scan in Figure 5 for $x_m = 9.6 \times 10^{-3}$ shows the absence of the endotherm at 253.3 K (which corresponds to the decomposition of clathrate hydrate).

(c) The Shape of the Relaxation Spectra of Process II. The relaxation of I_h doped with alkali hydroxides always shows the kind of behavior shown in Figure 2. The unusual feature with the C−C plot is the skewing on the lower-*F* side; eq 2 is only valid for the higher-*F* side (A similar trend, although to a lesser extent can also be seen in the case of KOH-doped I_c-(ACN) in the results of Yamamuro et al.[36] in the temperature range of 50−68 K, whereas it is not very much apparent in our results shown in Figure 6, which are taken at much higher temperatures). This means that the distribution of relaxation times is flatter on the lower-*F* side (or on the larger time scales) as discussed in the preceding section. This probably explains the effect of annealing on the size of the phase transformed during the low-*T* transition as observed by Tajima et al.[28]

Though the C−C plot has the advantage of giving first-hand information about the nature and magnitude of relaxation and the existence of other processes, it has the inherent disadvantage of not revealing the deviation from Debye behavior for nearly Debye processes, which can be presented better in a log ϵ'' vs log *f* plot.[39] Therefore, we have critically examined the relaxation data at several temperatures by plotting log ϵ'' against log *f* in the normalized form. The general trend is shown in Figure 11b−d for the case of doped I_h, I_c(ACN), and I_c(DXN). Also shown in Figure 11 are the data corresponding to pure I_h and ice clathrates. One striking feature of Figure 11 is the absence of high-frequency deviations often advocated[40] to be the universal feature of the glassy dynamics. The data on the high-frequency side follow a clear power law of the form[39]

$$\epsilon'' \propto f^{n-1} \quad \text{for} \quad f \gg f_m \tag{3}$$

with values of *n* ranging from 0 to 0.08 (one is also tempted to visualize another power law for $f \ll f_m$ but for the uncertainty caused by the presence of low-*F* spurs due to ionic conduction). The parameter *n* ($0 \le n < 1$) signifies the extent of cooperativity and is usually in the range 0.50−0.75 in supercooled plastic crystals[44,45] and liquids. The smaller values of *n* found in the present case indicate near absence of cooperativity among the molecules. Deviations from Debye behavior are larger on the low-*F* side but are more severe in doped I_c(ACN) both on the low-*F* and high-*F* sides as compared to that of doped I_c(DXN). At this juncture, it is interesting to note that in the former the enclathrated molecule is polar. It appears that there is a participation of this enclathrated molecule in the relaxation process making it broader.

(d) The Limiting High-*F* Dielectric Constant ϵ_∞. In the case of doped I_h, the value of ϵ_∞ is ∼3.0−3.2, which is not very much different from 3.0 found in case of pure I_h, and no additional process has been found on the higher-*F* side as in the case of pure I_h.[41] However, the situation is different in clathrate hydrates, which have an additional disorder due to the orientational mobility of the clathrated molecules.[11] Thus, one can expect an additional dielectric relaxation process if the enclathrated molecule is polar, and this process is expected[2,38] to occur in our LCR bridge frequency range at temperatures much below 77 K. In the case of pure I_c(ACN),[4,11] the ϵ_∞ is about 9.5 at 80.6 K, and this value is found to be 7.7 in LiOH-doped I_c(ACN) (Figures 6 and 7). The large difference of $\epsilon_\infty - 3.0$, which is a measure of the dielectric strength, indicates the existence of a high-*F* process due to the clathrated acetone molecules and is a measure of the disorder associated with these molecules. It is interesting to see that the dielectric strength corresponding to this process falls from 6.5 to 4.7 in the LiOH-doped hydrate. Thus, there seems to be a partial ordering of the enclathrated acetone molecules even at temperatures much above the low-*T* transition at 46.6 K (interestingly, the corresponding dielectric spectrum is broader as discussed in the previous section). This view is also supported by the specific heat, C_p, data of Yamamuro et al.[30]

(e) The Static Dielectric Constant (ϵ_0). In the case of I_h doped with nonelectrolytes[34] with $x_m \gg 10^{-3}$, all of the water molecules relax by only one process and the corresponding ϵ_0 values more or less tally with the ϵ_0 values corresponding to the single-crystal data of Kawada[12] on pure I_h (deviations from $\sim 1/T$ law are likely to occur on the low-*T* side because of the contraction of the sample from the electrodes or because of the development of pores and cracks as in a polycrystalline sample[2,34]). In the case of doped I_h or I_c(ACN), the ϵ_0 values do not change with temperature as rapidly as in the case of pure I_h (or I_c(ACN)). This is not due to the development of pores and cracks in the sample. There is a tendency for ϵ_0 to saturate or decrease slightly on lowering the temperature indicating a partial proton ordering (premonitory effect) even at temperatures a few tens of degrees above the low-*T* transition. A comparison of the ϵ_0 values of I_c(ACN) shown in Figure 9 with that given in ref 36 indicates a large mismatch, although the corresponding relaxation rates agree quite well with each other. This aspect needs an elaborate experimental clarification.

(f) The *T* Dependence of f_m. In the case of alkali hydroxides, some of the log f_m vs $1/T$ curves (Figures 3, 8, and 10) are so flat that, if fitted to eq 1, they yield an apparent activation energy of 1−19 kJ/mol with f_0 values far below that of the lattice vibrational frequency. In this context, it is interesting to see that all of the log f_m vs $1/T$ curves in the case of I_h doped with nonelectrolytes[34] or other impurities[14,32] contain three temperature regions of interest. On the high-*T* side, all of the curves more or less merge with that of pure I_h for which the activation energy is about 53 kJ/mol, which is the sum of the energies required for generation of orientational defects and for molecular reorientation by the motion of these defects.[14] On lowering the temperature, the number of intrinsically generated defects decreases, and hence, the mechanism switches over to the

extrinsic one, in which again the observed activation energy is the sum of the energies required from the extrinsic defect generation and its diffusion in a way as discussed by Johari and Whalley.[14] The middle temperature region with a low apparent activation energy is the crossover region.

Thus, it is tempting to attribute process II to the middle-*T* region[34] in which simple diffusion of defects guides the relaxation. However, it should be noted that the f_m values show peaks as in Figure 3 and have a tendency to approach the intrinsic process at higher temperatures. Because of this phenomena, it is not clear to us at this point of time whether the peaks are due to the onset of solidus melting or due to the crossover of the mechanism from that of Bjerrum[15] to that dominated by ionic impurities as advocated by Bilgram and Gränicher.[43]

Conclusions

(i) Our study supports the earlier view[28] that the alkali hydroxide dopants are very effective in catalyzing the low-*T* phase transition. Our studies show that the alkali ion and hydroxyl ion exert an influence over a surrounding region (domain) by way of their polarity. The amount of phase transformed during the low-*T* phase transition is determined by the number of these domains and hence is expected to be limited to the solid solubility, which in turn is severely restricted because of the size of the alkali ion.

(ii) The nature of the relaxation in ices or ice clathrates (both doped and undoped) is not cooperative and is determined mainly by the defects. And hence, it is doubtful whether this group of substances should really be categorized[28] as "glasses".

(iii) In view of the catalyzing action of the ionic impurities, a reexamination of the solid−liquid phase diagrams in the presence of alkali hydroxides should be interesting. Similarly, in our preliminary study on water−2-propanol binary, the long-lived metastable clathrate structure suspected to be of type I earlier has not been found in our dielectric study in the presence of KOH dopant. Thus, the PD diagram studies in the presence of these dopants may give some new and interesting results.

Acknowledgment. The Departmental Special Assistance (DSA) from UGC, India, is gratefully acknowledged.

References and Notes

(1) Franks, F. In *Water: A Comprehensive Treatise*; Franks, F., Ed.; Plenum: New York, 1972; Chapter 4, p 115.
(2) Davidson, D. W. In *Water: A Comprehensive Treatise*; Franks, F., Ed.; Plenum: New York, 1973; Vol. 2.
(3) Jeffrey, G. A. *Inclusion Compounds I*; National Research Council of Canada, Academic Press: London, 1984; p 135.
(4) Murthy, S. S. N. *J. Phys. Chem. A* **1999**, *103*, 7927.
(5) Blake, D.; Allamandola, L.; Sandford, S.; Hudgins, D.; Freund, F. *Science* **1991**, *254*, 548.
(6) Hasted, J. B. *Aqueous Dielectrics*; Chapman and Hall: London, 1973.
(7) Suga, H. *Pure Appl. Chem.* **1983**, *55*, 427.
(8) Suga, H. *J. Chim. Phys.* **1985**, *82*, 275.
(9) Pauling, L. *J. Am. Chem. Soc.* **1935**, *57*, 2680.
(10) Haida, O.; Matsuo, T.; Suga, H.; Seki, S. *J. Chem. Thermodyn.* **1974**, *6*, 815.
(11) Gough, S. R.; Hawkins, R. E.; Morris, B.; Davidson, D. W. *J. Phys. Chem.* **1973**, *77*, 2969.
(12) Kawada, S. *J. Phys. Soc. Jpn.* **1978**, *44*, 1881.
(13) Johari, G. P.; Jones, S. J. *J. Chem. Phys.* **1975**, *62*, 4213.
(14) Johari, G. P.; Whalley, E. *J. Chem. Phys.* **1981**, *75*, 1333.
(15) Bjerrum, N. *Science* **1952**, *115*, 385.
(16) Auty, R. P.; Cole, R. H. *J. Chem. Phys.* **1952**, *20*, 1309.
(17) Worz, O.; Cole, R. H. *J. Chem. Phys.* **1969**, *51*, 1546.
(18) Kelly, D. J.; Salomon, R. E. *J. Chem. Phys.* **1969**, *50*, 75.
(19) Ueda, M.; Matsuo, T.; Suga, H. *J. Phys. Chem. Solids* **1982**, *43*, 1165.
(20) Onsager, L.; Dupuis, M. *Electrolytes* Pergamon Press, Inc.: London, 1962.
(21) Onsager, L.; Runnels, L. K. *J. Chem. Phys.* **1969**, *50*, 1089.
(22) Lonsdale, K. *Proc. R. Soc. London, Ser. A* **1958**, *247*, 424.
(23) Gough, S. R.; Davidson, D. W. *J. Chem. Phys.* **1970**, *52*, 5442.
(24) Yamamuro, O.; Oguni, M.; Matsuo, T.; Suga, H. *J. Phys. Chem. Solids* **1987**, *48*, 935.
(25) Davidson, D. W.; Ripmeester, J. A. *Inclusion Compounds III*; National Research Council of Canada, Academic Press: London, 1984; p 67.
(26) Kuratomi, N.; Yamamuro, O.; Matsuo, T.; Suga, H. *J. Chem. Thermodyn.* **1991**, *23*, 485.
(27) Yamamuro, O.; Suga, H. *J. Therm. Anal.* **1989**, *35*, 2025.
(28) Tajima, Y.; Matsuo, T.; Suga, H. *J. Phys. Chem. Solids* **1984**, *45*, 1135.
(29) Yamamuro, O.; Oguni, M.; Matsuo, T.; Suga, H. *J. Phys. Chem. Solids* **1988**, *49*, 425.
(30) Yamamuro, O.; Kuratomi, N.; Matsuo, T.; Suga, H. *Solid State Commun.* **1990**, *73*, 317.
(31) Kuratomi, N.; Yamamuro, O.; Matsuo, T.; Suga, H. *J. Therm. Anal.* **1992**, *38*, 1921.
(32) Kawada, S. *J. Phys. Soc. Jpn.* **1972**, *32*, 1442.
(33) Sakabe, Y.; Ida, M.; Kawada, S. *J. Phys. Soc. Jpn.* **1970**, *28*, 265.
(34) Murthy, S. S. N. *Phase Transitions*, in press.
(35) Yamamuro, O.; Matsuo, T.; Suga, H. *J. Inclusion Phenom.* **1990**, *8*, 33.
(36) Yamamuro, O.; Kuratomi, N.; Matsuo, T.; Suga, H. *J. Phys. Chem. Solids* **1993**, *54*, 229.
(37) Hill, N. E.; Vaughan, W. E.; Price, A. H.; Davies, M. *Dielectric properties and molecular behaviour*; Van Nostrand Reinhold: London, 1969.
(38) Gough, S. R.; Ripmeester, J. A.; Davidson, D. W. *Can. J. Chem.* **1975**, *53*, 2115.
(39) Jonscher, A. K. *Dielectric relaxation in solids*; Chelsea Press: London, 1983.
(40) Dixon, P. K.; Wu, L.; Nagel, S. R.; Williams, B. D.; Carini, J. P. *Phys. Rev. Lett.* **1990**, *65*, 1108.
(41) Johari, G. P. *J. Chem. Phys.* **1976**, *64*, 3998.
(42) Kawada, S. *J. Phys. Soc. Jpn.* **1979**, *47*, 1850.
(43) Bilgram, J. H.; Gränicher, H. *Phys. Condensed Matter* **1974**, *18*, 275.
(44) Tyagi, M.; Murthy, S. S. N. *J. Chem. Phys.* **2001**, *114*, 3640.
(45) Murthy, S. S. N. *Thermochim. Acta* **2000**, *359*, 143.